

A NUMERICAL METHOD TO PREDICT THE LIFT OF AIRCRAFT WINGS AT STALL CONDITIONS

Marcos A. Ortega

ITA – Technological Institute of Aeronautics
CTA-ITA-IEA, São José dos Campos, SP, 12228-900
ortega@ita.br

Roberto M. Girardi

ITA – Technological Institute of Aeronautics
CTA-ITA-IEA, São José dos Campos, SP, 12228-900
girardi@ita.br

Paulo S. Komatsu

EMBRAER – Brazilian Aircraft Corporation
Av. Brig. Faria Lima, 2.170, São José dos Campos, SP, 12227-901
pkomatsu@embraer.com.br

Abstract. During the early stages of an aircraft conception and design, fast and reliable numerical tools to evaluate the capabilities of a new configuration are mostly needed. The main aim of this work is to provide one such a tool to predict the aerodynamic characteristics of wings up to stall conditions. The approach corresponds to using a three-dimensional non-linear potential Weissinger basis upon which two-dimensional viscous data at some stations are inputted. A very effective iteration strategy is then established, which provides convergence between calculated and realistic data at these stations. The paper focusses on the general discussion of the method and its application to some test cases.

Keywords: Wing's High Lift, Weissinger Method, Viscous-Potential Iteration

1. Introduction

At takeoff and landing, airplanes' wings are to be positioned at high angles of attack, in order to gain more lift and therefore to compensate for the usually low velocities at those phases of the flight mission. On the other hand, at high angles of attack, the flow gets prone to detaching from the upper surface of the wing, what might result in a severe drop in lift and a rise in drag — a condition known as the wing stall. The solution for these specific demands was discovered at the very dawn of the aeronautical industry, and corresponds to the introduction of the so called high-lift devices — basically, some proper combination of slats and flaps. Besides this very fundamental point of aerodynamic performance, there is also today an ever increasing attention to reducing the complexity and weight of the high-lift systems for given maximum lift levels. This, because multi-element-high-lift systems have a significant impact both in manufacturing and maintenance costs as well as they are vital in the extension of the operational envelope of a new aircraft. Just to cite one example, an increase of 1.0% in the maximum lift coefficient corresponds to an increase in payload of 22 passengers or about 2000 kg for a fixed approach speed on landing of a large twin engine transport (Meredith, 1993). Therefore, an accurate prediction of the flow about the wing in those conditions is much needed.

Traditionally, design is done in a sequential fashion (Nield, 1995), and the high-lift device is tackled near the end of the process where much of the aircraft geometry has already been committed. Typically, 90% of the overall costs are committed at the initial 10% of the design process (Davis, 1996). Focussing on the high-lift devices early at the beginning might produce simpler high-lift systems, which can very well translate in significant reduction in production costs. Besides, early addressing of these lifting mechanisms might also mean profiting in derivative aircraft performance, as well as avoiding unpleasant surprises, as for example, to discover that, after the configuration is basically frozen, the required CL_{max} corresponds to a certain high-lift configuration that does not fit in the allotted space. (Observe that we shall use the symbol CL to indicate the lift coefficient of the (three-dimensional) wing, while Cl will be used to indicate the local coefficient at a certain (two-dimensional) station along the span). On the other hand, if one is to evaluate a proposed high-lift system at the conceptual design stage, the tool to be used has to be reliable, and overall very fast, in order to produce results that can be duly aggregated to the configuration. This paper suggests a numerical prediction strategy that bears these most wanted features.

The idea of using potential tools to evaluate the stall conditions of finite wings is an old one. A traditional method (Sivells and Neely, 1947) compares the spanwise distribution of the potential-obtained local lift coefficient at the wing with the spanwise values of Cl_{max} of the profiles at each station. When the two distributions firstly touch, one considers that the wing is starting to stall. The angle of touching is taken as the maximum angle of attack, and, at this position, the CL of the wing is calculated and considered as the maximum value of the wing lift (lift at stall). This simple approach works rather well for straight wings mounted with the same profile from root to tip. But, for more sophisticated forms — swept wings, with breaks and different profiles along the span —, the accuracy of the method is poor. Recently, a very attractive methodology was devised by a group of the University of California, Davis, led by prof. C. P. van Dam. This group has been working steadily in the area of high-lift systems development and

optimization, with a special view to the early stages of the aircraft design (Pepper and van Dam, 1996, van Dam et al., 2001, van Dam, 2002). The proposed aerodynamic strategy consists of, say, a potential basis, that in this case is constituted by an extended lifting-line method, mostly known in the literature as method of Weissinger (Weissinger, 1947, Schlichting and Truckenbrodt, 1979). The potential tool is coupled with viscous flow data relative to a number of profiles specifically chosen at some stations along the span (van Dam et al., 2001). At this point an iterative procedure is triggered, whose aim is to approximate the value of the local lift coefficient obtained by the potential calculation, to the values of the realistic airfoil lift coefficient at these specified positions. After convergence, the value of the wing lift is obtained by integrating the local lift values. The procedure is repeated for a range of angles of attack that reaches beyond the stall condition.

The present work corresponds to the initial stages of a broader research plan, whose final aim is to obtain accurate values of the lift, moment and drag coefficients at stall conditions. The ultimate idea is to test complete configurations, that is, modern swept wings, including, eventually, effects of flaps and/or slats, fuselage, engine nacelles, horizontal tail, etc.. The technique can also be adapted to predict wind tunnel wall influences. Because the main drive behind this effort is the application of the method in the early stages of a new aircraft configuration definition, including the conceptual phase, the numerical code has to be flexible and especially quick. Therefore, at least to start with, we had in mind following the main suggestions of prof. van Dam's program. We then developed a potential basis, the same Weissinger's method, and coupled to it an iteration technique by means of which we introduce realistic viscous profile data. But the methodology to be presented in this paper has some definite differences when compared to the literature (van Dam et al., 2001). For reasons that will become clear in the following, another cycle of convergence, that we have called the "external loop", was introduced, in order to guarantee the value of the initial angle of attack. The internal loop (the only one that appears in van Dam's work), as we have called it, consists of the iteration that tries to equate the calculated and realistic local lift coefficients. In the following, we shall give the most important details of the method at its present state, and some results already obtained with the resulting numerical code.

2. The Algorithm

2.1. The Extended Lifting-Line Method

The first successful attempt to model the three-dimensional finite wing was done by Prandtl and is known in the literature as the "lifting-line method". It works well for wings of large aspect ratio and straight quarter-point lines. An extension of the lifting-line idea, that can be applicable to arbitrary wings and lifting surface arrangements, is known as the three-quarter-point method (Schlichting and Truckenbrodt, 1979). In this case the wing is replaced by a collection of elementary wings, each one modeled by an elementary horse-shoe vortex — see Fig. 1. The bound vortex segments are positioned along the quarter-point line. Because each elementary wing is represented by a single elementary vortex, the kinematic flow condition — the basic boundary condition of potential theory, whereby the surface normal velocity component is zero — can be satisfied at one point of the chord only. This point is placed on the three-quarter-chord station measured from the leading edge, and this convenient position is a consequence of the theorem of Pistoletti (Schlichting and Truckenbrodt, 1979, p. 78). This method was developed in detail and applied particularly by Weissinger (1947). It is well fit to wings of any planform and aspect ratio, and gives the lift distribution over the span from which total lift, rolling moment, induced drag, and, approximately, pitching moment are obtained.

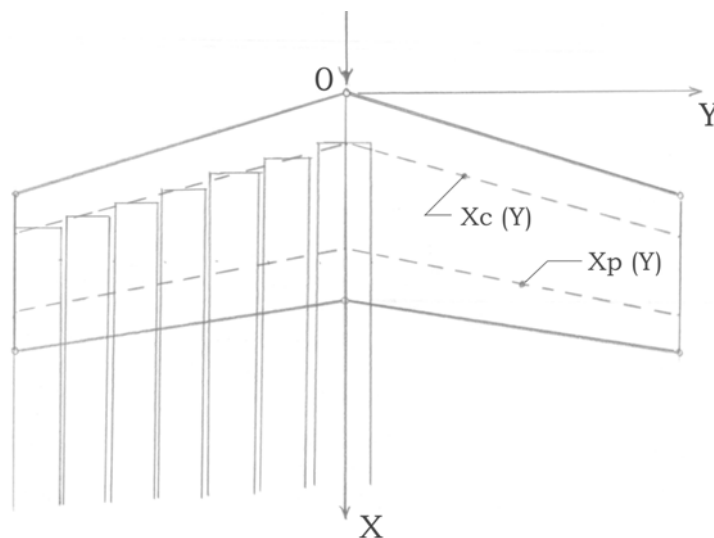


Figure 1. Wing modelling by a distribution of elementary vortices.

The extended lifting-line method (as well as other incompressible schemes) can be also applied in the compressible subsonic régime, and then Mach number effects can be accounted for, by the application of the so called Prandtl-Glauert rule (Schlichting and Truckenbrodt, 1979). After the problem is solved the total lift can be obtained by direct integration of the load distribution. With the calculated circulation one can work at the Trefftz plane to obtain the induced velocities and, in consequence, the induced drag. If the profile drag of the individual airfoil sections is available, it can be integrated along the span, added to the induced drag and the result is the total drag of the wing. The pitching moment can also be obtained by integration after one has calculated the individual moments at each station. In the Weissinger method the lifting surfaces are reduced to flat plates. Anyhow, any profile form can be used, and its characteristics will be felt through the repositioning of the control points as function of the particular lift slope, as well as the angle of attack that is referred to the zero-lift line. By doing so, the angle of zero lift of the airfoil is taken into account.

Observe Fig. 1. It depicts the discretization of the original wing in a certain number of elementary wings. To each elementary wing we attribute a value of circulation that we shall denote by γ_j . These are the basic parameters to be determined. To obtain the system of algebraic equations the kinematic boundary condition is applied to each control point, which are located on the three-quarter-point line. Enforcing boundary conditions requires the obtention of the induced velocity at the control points. In doing so we obtain the influence coefficients, which depend basically upon the geometry of the wing. These coefficients are then arranged in matrix form. The product of this matrix by the vector of unknown γ_j 's must balance the vector of angles of attack. Solution of this system gives the value of the circulation for each of the elementary wings.

2.2. Strategy for the Calculation of the Maximum Lift

As we have already advanced at the introduction, a strategy to introduce realistic data in the algorithm has to be devised. These realistic data correspond to the C_l versus α curve of the two-dimensional airfoil at some pre-defined stations. Lift data of airfoils can be obtained from wind tunnel measurements or from some Navier-Stokes computer code. In either case, viscous effects play, evidently, a major role. Viscous effects are responsible for the non-linearity of the profile C_l versus α curve. The main aim here is to devise a mechanism that will "transport" this non-linearity to the potential tool already available. Following van Dam et al. (2001), we shall adopt a mechanism that corresponds to an iteration procedure. Two-dimensional viscous airfoil data shall be compiled in a data bank and read by the code at the start. At least two stations have to receive these information: the root and the tip sections. The lift-curve slope, C_{l_α} , and the zero-lift angle of attack, α_o , are then calculated for the, say, "realistic stations", that is, for the number of stations that received the two-dimensional viscous data. These values can be duly interpolated to the other stations, and, then, the potential subroutine is called for the first time. After this initial three-dimensional calculation a load distribution along the span is obtained. Then the following iterative procedure is performed for each of the realistic sections (van Dam et al., 2001).

- 1) Estimate a new value of the local "effective" angle of attack for each of the realistic sections:

$$\alpha_{local} = \frac{C_{l_w}}{C_{l_\alpha}} + \alpha_o - \Delta\alpha_{visc}$$

where C_{l_w} is the calculated (by the potential subroutine) local lift coefficient and $\Delta\alpha_{visc}$ is a viscous correction (step 3).

- 2) Enter the two-dimensional profile data for the station with the value of α_{local} and through interpolation estimate the value of $C_{l_{visc}}$.

- 3) If $|C_{l_{visc}} - C_{l_w}|$ is less than a certain pre-established tolerance, stop the process. Otherwise, determine an angle correction for each realistic section, $\Delta\alpha_{visc}$, such that, for the local angle of attack the potential lift coefficient equals $C_{l_{visc}}$:

$$\Delta\alpha_{visc} = \frac{C_{l_{visc}} - C_{l_w}}{C_{l_\alpha}}$$

Figure 2 shows graphically the concept of $\Delta\alpha_{visc}$.

- 4) The angles of attack at these pre-determined stations should be corrected with the values of $\Delta\alpha_{visc}$, and with this new angle of attack distribution call again the potential subroutine.

- 5) Return to step 1, and repeat the procedure until $|C_{l_{visc}} - C_{l_w}|$ is less than the given tolerance for all stations.

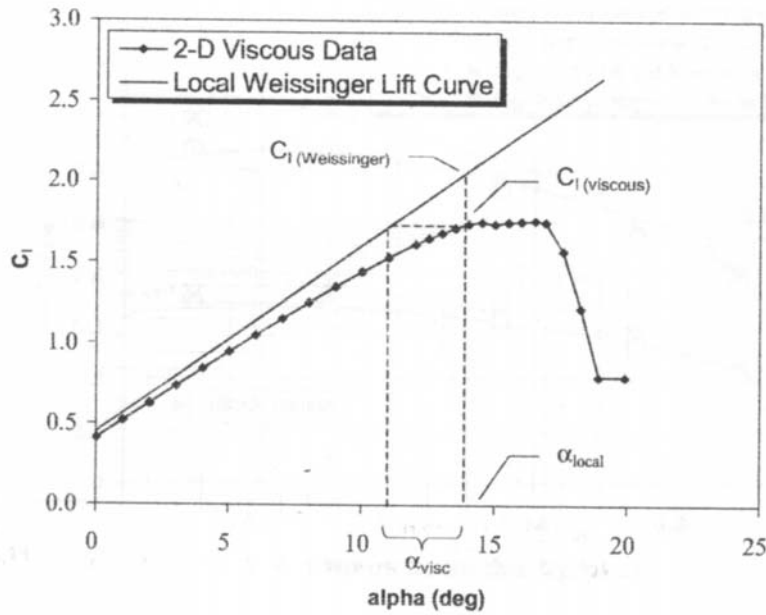


Figure 2. Definition of a viscous correction angle.

The above procedure was incorporated to our codes. Soon, some modifications showed up to be necessary. Some kind of mechanism had to be introduced in order to define the value of $\Delta\alpha_{visc}$ for the stations that not received the viscous information. We decided by a simple linear interpolation between successive stations. Besides, it was necessary to introduce a relaxation parameter for the values of $\Delta\alpha_{visc}$, because convergence was not trivial. But, by far, the most amazing feature is that the above procedure simply did not work. We tried exhaustively to obtain any meaningful result, but did not succeed, in spite that the literature (van Dam et al., 2001) informs that the approach is reliable. After a thorough analysis of the whole process, we arrived at a diagnostic. Basically, what happens can be understood by observing figure 2. When one calculates the first value of $\Delta\alpha_{visc}$ a kind of a step of a ladder is formed. In the second trial another step is formed, in continuation of the first, between the potential and viscous lift values distributions. In subsequent iterations one “goes down the ladder” in the direction of small values of α , where finally convergence is attained because the curves get closer to each other. But, at the end, when a converged solution is finally obtained, the value of α is in general too small. Suppose that we wanted to calculate the lift value for a geometric angle of attack equal to 12° . One can, at the end, obtain a solution, but for a final value of $\alpha=2^\circ$, and this has completely changed the initial positioning of the wing.

To circumvent the problem we proceeded as follows. The above iterative scheme was considered as an inner loop, and an outer convergence loop was introduced. This new loop works according to the following steps:

- 1) Run the code to perform an inner loop. In order to avoid the ladder effect the first collection of viscous lift values that are obtained by interpolation is frozen. So, the objective of the inner convergence process is now fixed, and the local potential loads are made to converge to these values.
- 2) After an inner loop is finished, the initial value of the geometric angle of attack is re-composed. This is necessary because, in spite of the frozen values introduced in step 1, the final local geometric angles of attack always change. The approach is the following: calculate the mean value of the geometric angles of attack along the span, by summing up the local values and dividing the sum by the number of elementary wings. The difference between the given initial angle and this mean is summed up to every local angle of attack.
- 3) Call the potential subroutine and obtain a new value for the total lift of the wing. Calculate the difference $|CL_{n+1} - CL_n|$, where n is the counter of the external cycles. If this difference is less than a certain pre-established tolerance the process is stopped. Otherwise the process returns to step 1.

This new scheme, now comprising an inner and an outer loop, worked quite well and the ladder effect was completely removed. By applying the methodology for a complete angle-of-attack sweep, values of the maximum lift and angle of attack can be determined. It is important to keep in mind that three external parameters play an important role in the scheme: two accuracy reference parameters (for the inner and outer loops) and a relaxation coefficient. In the next section some applications are presented that validate the proposed procedure.

3. Results and Discussion

The objective of the first case is to test the accuracy of the Weissinger method alone, that is, we want to validate the potential basis. A 45° swept wing was used for comparison purposes. For this case there is both experimental (Martina, 1956) as well as numerical (also potential) data (Paris, 1999). The main characteristics of the wing can be seen in Fig. 3. The wing has an aspect ratio of 8.02 and is mounted high on a cylindrical portion of the fuselage.

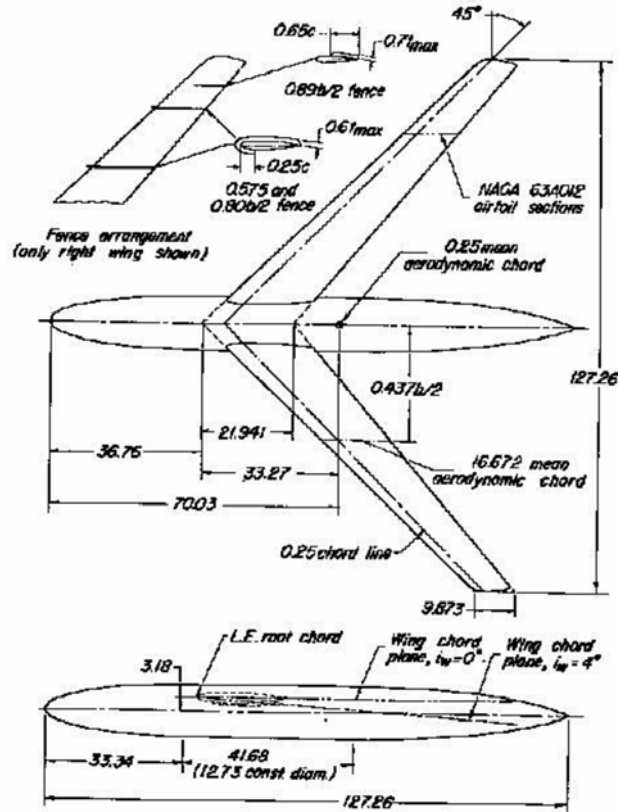


Figure 3. Wing-body combination.

The version of the potential code used in this particular study incorporates also the fuselage effect. The fuselage is modeled as an infinite cylinder, and the influence is felt by the wing through a positive induced effect, which can be calculated by considering potential flow about a circular cylinder. This induced effect is given by a distribution of angle φ given by

$$\varphi = \tan^{-1} \left\{ \frac{\sin \alpha_B \cos \alpha_B \left[\frac{R^2 (y^2 - z^2)}{(y^2 + z^2)^2} \right]}{1 + \sin^2 \alpha_B \left[\frac{R^2 (y^2 - z^2)}{(y^2 + z^2)^2} \right]} \right\}$$

where α_B and R are the fuselage angle of attack and radius, respectively, and y and z are Cartesian coordinates. Figure 4 shows comparison of data for a geometric angle of attack equal to 8.8°. As can be seen, the results predicted by the Weissinger method with and without fuselage effect compare very well with both experimental and numerical data. We have also run a number of other test cases and the results of the Weissinger platform were always very accurate.

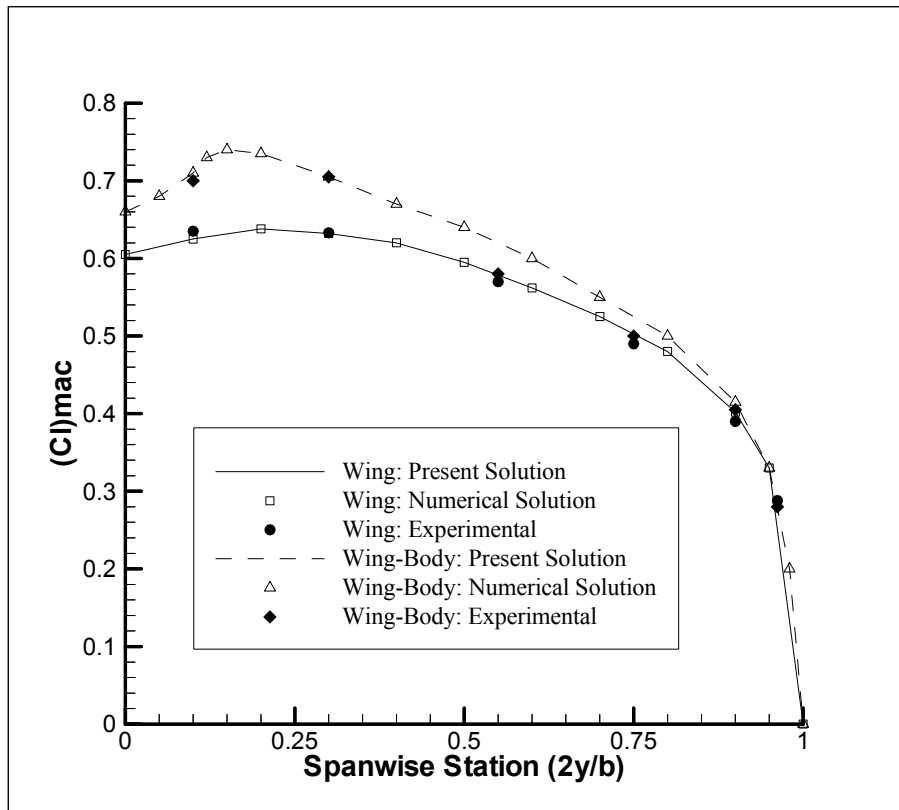


Figure 4. Spanwise load distribution for the wing-body combination.

We pass now to the discussion of the maximum lift prediction results. The reference is the work of Sivells (1947). The author has tested in the wind tunnel three wings, all with the same planform, with a straight quarter-point line, aspect ratio equal to 9, with a ratio of root chord to tip chord of 2.5, and with a dihedral angle of 3°. Two of the wings used the profile NACA 65-210 (all along the span), one without washout and the other with 2° washout, and the third was constructed with the NACA 64-210, and with 2° washout. Figures 5, 6 and 7, show the comparison of predicted and experimental values. Overall agreement is quite good, nonetheless, two aspects are worth noting. When compared to the experiment, the numerical scheme is lagging slightly the perception of the stalling point, especially in the value of the stalling angle. For the NACA 65-210 wing, without washout (Fig. 5), the lift coefficient and stalling-angle values are 1.23, 1.249, 13.5°, and 14°, respectively, for experimental and numerical evaluations. The error for the maximum lift is 1.5% and for the angle of attack is 3.7%. On the other hand it is important to bear in mind that experimental values of the stalling angles were obtained using the wool tufts technique (Sivells, 1947), an approach that does not present a high degree of accuracy. The other point to be made is relative to the tendency shown by the distribution of lift values for the cases where washout is present (Figs. 6 and 7). The predicted values are slightly less than the experimental ones, even at the linear stretch of the $CL\alpha$ curve. This simply did not happen for the case without washout, as the reader can grasp from Fig. 5. At the time of writing this article we were trying to figure out what were the causes for these deviations. We believe that the distortion at the stalling region is related to the restoration of the initial angle of attack by the mean approach. Because, by doing so, the vector of angles of attack of the matricial equation is being altered. We are convinced that this is not the optimum procedure, therefore, we still hope to improve the algorithm further. In relation to the second problem, values of lift less than the experimental ones for washouts different from zero, we still do not have a clue to pursue.

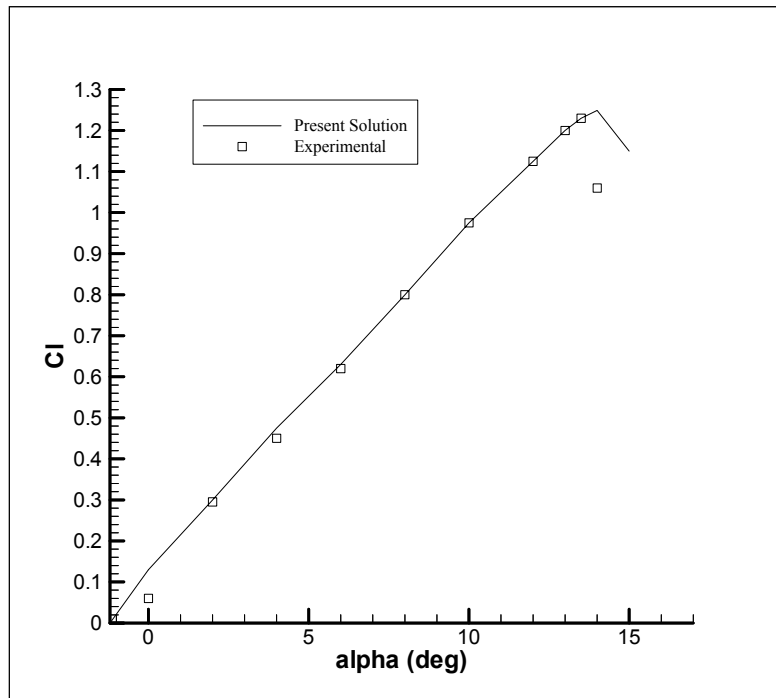


Figure 5. Comparison of calculated and experimental lift curves of wing having NACA 65-210 airfoil sections. Washout, 0°, Reynolds number, 4.5×10^6 , Mach number, 0.17.

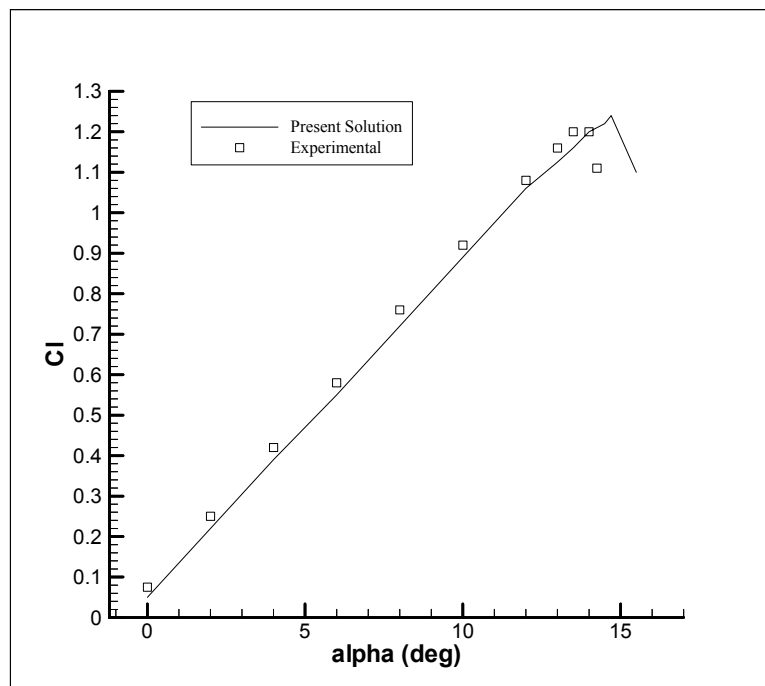


Figure 6. Comparison of calculated and experimental lift curves of wing having NACA 65-210 airfoil sections. Washout, 2°, Reynolds number, 4.5×10^6 , Mach number, 0.17.

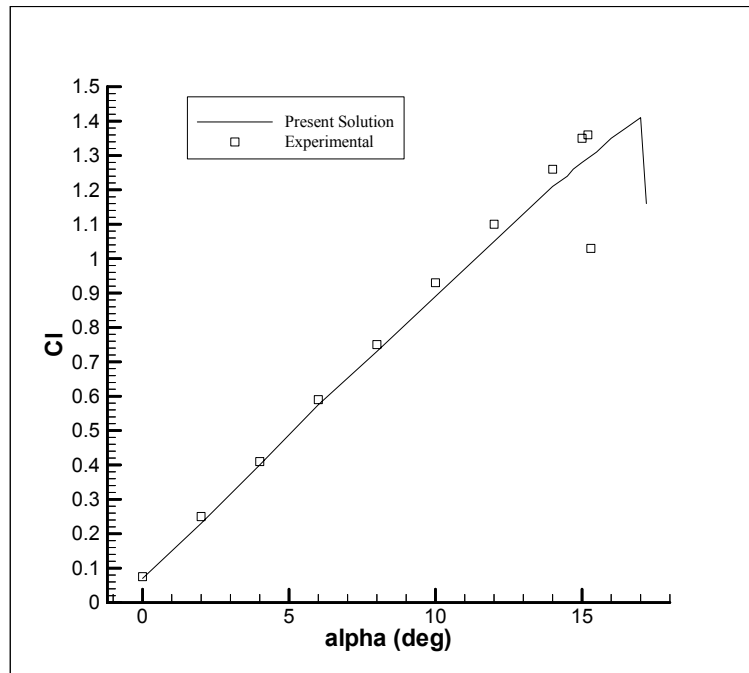


Figure 7. Comparison of calculated and experimental lift curves of wing having NACA 64-210 airfoil sections. Washout, 2°, Reynolds number, 4.5×10^6 , Mach number, 0.17.

The method proposed can also be used for other important and instructive aerodynamic studies. Let us consider the wing with NACA 65-210, without washout. Figures 8, 9, 10 and 11 show the distribution of local lift coefficient along the span, just before and just after the stall establishment. The reader can appreciate immediately the negative effect of the process. Figure 8, $\alpha=13^\circ$, shows a typical spanwise load distribution for tapered (and also swept) wings. Figure 9, for which the angle of attack is equal to 13.6° , is very instructive, because it corresponds to the onset of stall. It is the first time that some stations of the wing are reaching the lifting limit of the two-dimensional profile that, for this case is equal to 1.29 (a dotted line marks this limit). Evidently, the station cannot sustain a C_l greater than 1.29, and the result is that the local load falls. With the growing of the angle of attack we reach a condition represented in Fig. 10, for which many stations along the wing are stalled, but yet the wing itself is not, because the total lift coefficient of the wing for $\alpha=13.9^\circ$ is still greater than that for $\alpha=13.6^\circ$. This is still so because the load distribution is larger, in the mean, for $\alpha=13.9^\circ$ when compared to $\alpha=13.6^\circ$ (see also Fig. 5).

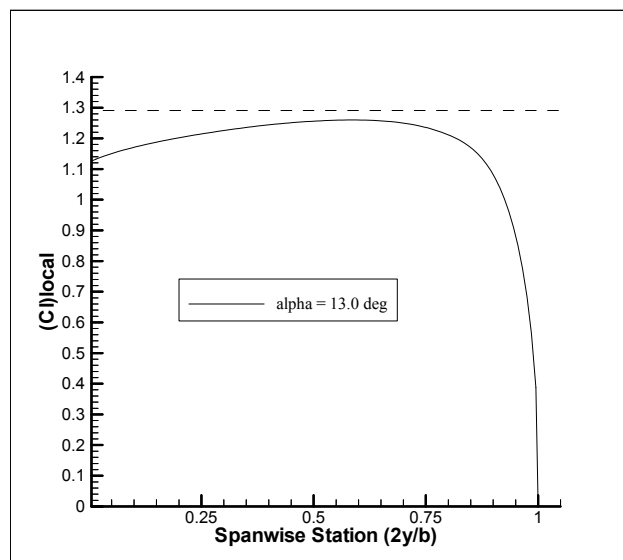


Figure 8. Spanwise load distribution for wing having NACA 65-210 airfoil. Before stall.

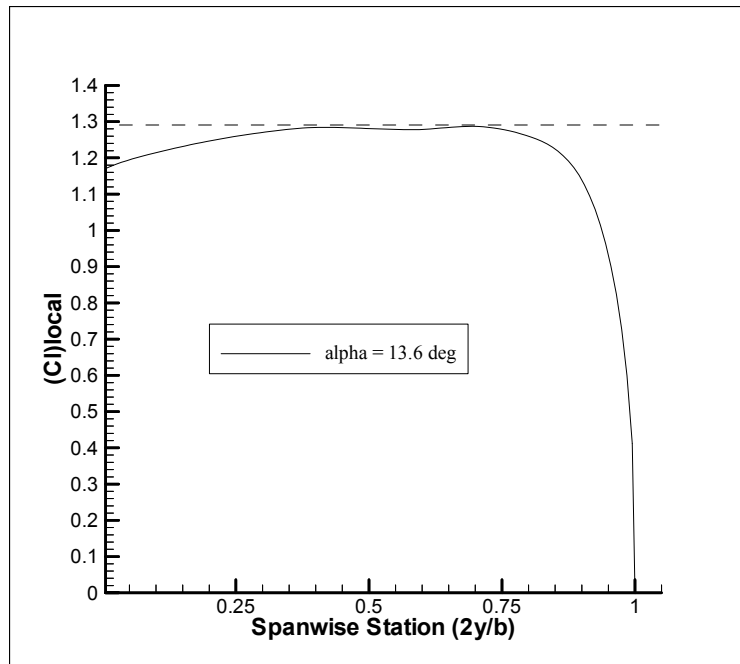


Figure 9. Spanwise load distribution for wing having NACA 65-210 airfoil. Stall onset.

Stalling is finally established for $\alpha=14.1^\circ$, when the total lift starts to diminish. It is important to bear in mind that the load distribution represented in Fig. 11 does not represent a good solution anymore. Because, according to Kroeger and Feistell (1976), care should be exercised in applying nonlinear lifting-line methods to poststall calculations.

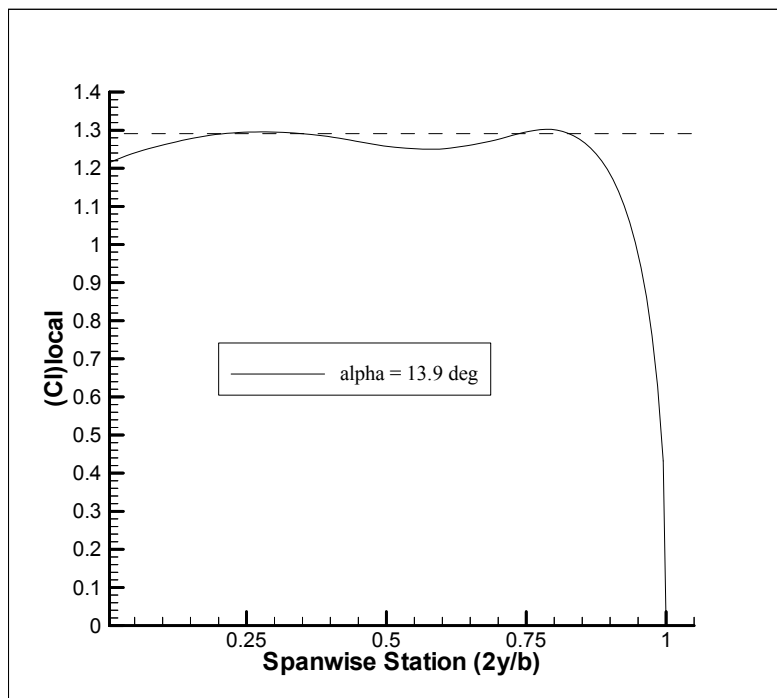


Figure 10. Spanwise load distribution for wing having NACA 65-210 airfoil. Stall establishment.

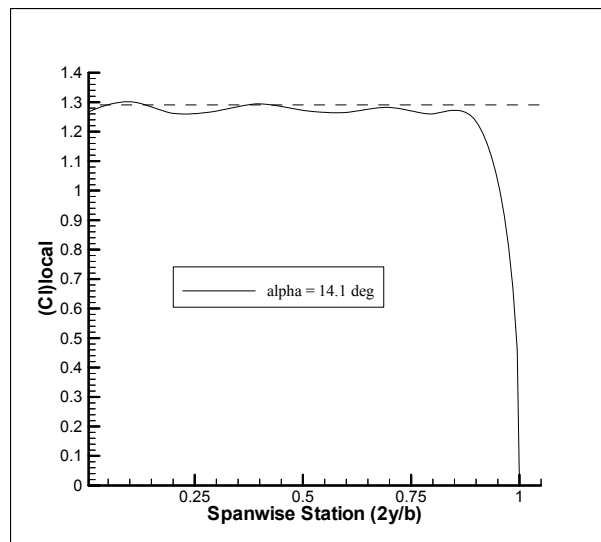


Figure 11. Spanwise load distribution for wing having NACA 65-210 airfoil. After stall.

4. Conclusions

A methodology for the prediction of aerodynamic characteristics of a finite wing at stall conditions is presented. The new scheme introduces another iterative cycle, that was called “the outer loop”, in contrast to the work of van Dam and co-workers (van Dam et al., 2001). This new strategy was necessary in order to maintain the initial value of the geometrical angle of attack. The scheme is robust and convergence is attained in few cycles, even for angles of attack beyond the stalling condition. The results can be considered quite good, in spite that there are still some points to be settled, in order to improve accuracy even further. Presently, we are working on these points and at the same time extending the methodology for wings with flaps.

5. Acknowledgments

The authors would like to point out that this study was supported and funded jointly by FAPESP, the State of São Paulo Foundation for the Research Support, and EMBRAER, Brazilian Aircraft Corporation.

6. References

- Davis, P., 1996, “Industrial Strength Optimization at Boeing,” SIAM News, Vol. 29, No. 1.
- Kroeger, R. A., and Feistell, T. W., 1976, “Reduction of Stall-Spin Entry Tendencies Through Wing Aerodynamic Design,” Society of Automotive Engineers, Paper 760481.
- Martina, A. P., 1956, “The Interference Effects of a Body on the Spanwise Load Distributions of Two 45° Sweptback Wings of Aspect Ratio 8.02 from Low-Speed Tests,” NACA TN 3720.
- Meredith, P., 1993, “Viscous Phenomena Affecting High-Lift Systems and Suggestions for Future CFD Development,” High-Lift System Aerodynamics, AGARD CP 515, pp.19-1--19-8.
- Nield, B. N., 1995, “An Overview of the Boeing 777 High-Lift Aerodynamic Design,” Aeronautical Journal, Vol. 99, No. 989, pp. 361-371.
- Paris, J. K., 1999, “Advancements in the Design Methodology for Multi-Element High-Lift Systems on Subsonic Civil Transport Aircraft,” M.Sc. Thesis, Dept. of Mechanical and Aeronautical Engineering, Univ. of California, Davis.
- Pepper, R. S. and van Dam, C. P., 1996, “Design Methodology for High-Lift Systems on Subsonic Aircraft,” NASA CR 202365, Aug. 1996.
- Schlichting, H. and Truckenbrodt, E., 1979, “Aerodynamics of the Airplane”, McGraw-Hill International Book Company, New York.
- Sivells, J. C., 1947, “Experimental and Calculated Characteristics of Three Wings of NACA 64-210 and 65-210 Airfoil Sections with and without 2° Washout,” NACA TN 1422.
- Sivells, J. C. and Neely, R. H., 1947, “Method for Calculating Wing Characteristics by Lifting-Line Theory Using Nonlinear Section Lift Data,” NACA TN No. 1269.
- van Dam, C. P., 2002, “The Aerodynamic Design of Multi-Element High-Lift Systems for Transport Airplanes,” Progress in Aerospace Sciences, Vol. 38, pp. 101-144.
- van Dam, C.P., van der Kam, J.C. and Paris, J. K., 2001, “Design-Oriented High-Lift Methodology for General Aviation and Civil Transport Aircraft,” Journal of Aircraft, Vol. 38, No. 6, pp. 1076-1084.
- Weissinger, J., 1947, “The Lift Distribution of Swept-Back Wings,” NACA TM 1120.